JOURNAL OF MATERIALS PROCESSING TECHNOLOGY 204 (2008) 520–521

available at www.sciencedirect.com

ScienceDirect

journal homepage: www.elsevier.com/locate/jmatprotec

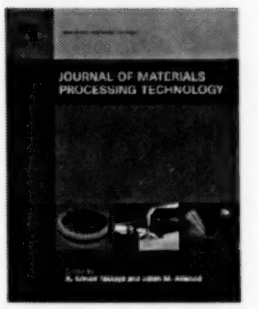

Author Index of Volume 204

Abbasi, M.H., 125
Abd El Aal, E.E., 139
Abd El Haleem, S.M., 139
Abed, K.M., 343
Ahmad, M.M.H.M., 350
Ahmad, Z.A., 279
Ak Azem, N.F., 221
Allwood, J.M., 290
Anawa, E.M., 22
Anderson, D., 269
Attar, A., 284
Audier, M., 248
Audy, J., 130
Axinte, D.A., 357

Babakhani, A., 192
Bataineh, O.M., 343
Bauer, R., 269
Bayraktar, E., 313, 440
Bhuiyan, N., 284
Bian, J., 481
Birlik, I., 221
Bouzid, W., 213
Bray, S., 48

Cadenas, M., 304
Cao, Y.Y., 357
Celik, E., 80, 221
Ceschini, L., 231
Cevik, A., 117
Ceylanoğlu, A., 264
Chang, Y., 481
Chen, C.-P., 419
Chen, D.-C., 419
Cheng, R.H., 502
Cramer, A., 103
Culha, O., 221

Dal Maso, U., 403
Dąbrowski, B., 199
Dąbrowski, J.R., 199
Das, S.K., 239
Daver, F., 397
Davim, J.P., 459, 469
Dey, P.K., 239
Du, G., 481
Duan, B.H., 111
Dubey, A.K., 412

Enayati, M.H., 125
Erenc-Sedziak, T., 465

Farahat, A.I.Z., 365
Faucheux, V., 248
Fernández, J.E., 304
Findik, F., 80

Gaitonde, V.N., 459
Galantucci, L.M., 403
Garrido, M.A., 304
Gerbeth, G., 103
Ghambri, M., 192
Ghosal, P., 434
Gibbons, G.J., 184
Godiwalla, K.M., 239
Gómez-del Río, T., 304
Görgülü, K., 264
Grądzka-Dahlke, M., 199
Grumbach, M., 313
Gupta, R., 397

Haerian, A., 192
Hansell, R.G., 184
Hassan, A.M., 343
He, S., 179
He, X.B., 111
Hegde, S.S., 239
Hong, S.-T., 486
Huang, B., 179
Hussain, L.B., 279

Işıkdağ, B., 34
Ito, K., 89

Jackson, K.P., 290
Jia, C.C., 111
Jiang, Z.Y., 152
Johnson, R.T., 486
Joo, H.U., 498
Jung, W.-S., 498

Kang, C.G., 8
Kang, F.W., 147
Kao, W.-C., 425
Kaplan, D., 313, 440
Karadge, M., 48
Karimzadeh, F., 125
Karnik, S.R., 459
Karunakaran, K.P., 384
Kim, B.-M., 8
Kim, H.S., 370
Koç, M., 370
Koksal, S., 80
Kopac, J., 94
Korosec, M., 94
Kosior, E., 397
Kowalczyk, M., 465
Koyama, H., 89
Kuboki, T., 162
Kulik, T., 465
Kumar, D.R., 70
Kumar, P., 59
Kumar, S., 59
Kumari, S., 434
Kuziak, R., 255

Lahrman, D., 486
Landert, M., 290
Lavender, C.A., 486
Lee, H.-D., 425
Lee, S.M., 8
Li, Z., 147, 179
Liang, H., 481
Liang, X., 465
Liu, W., 481
Liu, X.H., 152
Liu, Y., 179
Liying, Y., 492
Lladó, J., 1
Lou, Y., 327
Lu, Y., 513

Ma, J., 508
Manabe, K., 89
Mata, F., 469
Matoorian, P., 350
Mehrotra, S.P., 239
Michalski, J., 331
Moat, R., 48
Mohanrao, R., 434
Monteiro, E., 451
Morri, A., 231
Mousavi, T., 125
Murata, M., 162

Nishida, K., 162
Noh, M.Z., 279
Northwood, D.O., 327

Olabi, A.G., 22

Padmavathi, N., 434
Palanikumar, K., 469
Pan, C.T., 502

Elsevier B.V.
doi:10.1016/S0924-0136(08)00454-8

Pan, F., 111
Panda, S.K., 70
Paqueton, H., 313
Peiquan, G., 492
Percoco, G., 403
Petryk, H., 255
Pignard, S., 248
Preuss, M., 48

Qu, X.H., 111

Rapenne, L., 248
Ravi Kumar, D., 169
Rawson, M., 48
Ray, K.K., 434
Rodríguez, J., 304
Rouboa, A., 451

Sahoo, S.K., 206
Saï, L., 213
Sakaki, T., 162
Sambogna, G., 231
Sánchez, B., 1
Schmidt, F., 313
Schultz, R.W., 39
Shan, H.S., 59
Shen, J., 147
Shimizu, T., 89
Shouren, W., 492
Shringi, R., 384
Silberschmidt, V.V., 206
Singh, S.K., 169
Skoczylas, L., 331
Smith, M.T., 486
Stupkiewicz, S., 255
Subrahmanyam, J., 434
Sulaiman, S., 350
Sun, J., 481
Sun, J.F., 147

Tang, C.F., 111
Thomson, V., 284
Tieu, A.K., 152
Toparli, M., 221
Topçu, İ.B., 34
Turk, A., 221

Ulysse, P., 39

Wang, G.D., 152
Wang, H., 327
Wang, J., 425
Wang, J.-P., 425
Wang, J.S., 152
Wang, X., 481
Warkentin, A., 269
Wu, H., 179

Xu, B., 465
Xu, Y., 513

Yadava, V., 412
Yan, B., 475
Yan, L., 513
Yang, M., 89
Yang, R., 513
Yang, T., 481
Yang, Z., 513
Yigit, R., 80
Yilbas, B.S., 440
Yin, P., 513

Zghal, A., 213
Zhang, G.Q., 147
Zhang, W., 508
Zhang, Y., 475
Zhou, H., 475

JOURNAL OF MATERIALS PROCESSING TECHNOLOGY 204 (2008) 522–530

ELSEVIER

available at www.sciencedirect.com

ScienceDirect

journal homepage: www.elsevier.com/locate/jmatprotec

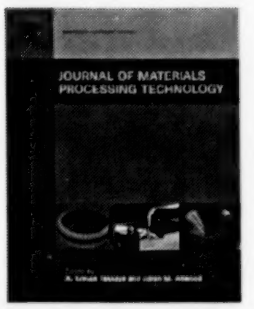

Subject Index of Volume 204

Abrasive effectiveness
Evaluation of continuous grinding tests on some marble and limestone units with silicon carbide and diamond type abrasives, 264
Adaptive feed
Chip thickness analysis for different tool motions. for adaptive feed rate, 213
Adhesion
Microstructural, thermal and mechanical properties of HVOF sprayed Ni–Al-based bond coatings on stainless steel substrate, 221
Ag nanoparticles
Synthesis of Ag nanoparticles by hydrolysis of Mg–Ag intermetallic compounds, 327
^{27}Al MAS NMR
Effect of carbon monoxide on the carbothermal reduction and nitridation reaction of alumina, 498
AlN
Effect of carbon monoxide on the carbothermal reduction and nitridation reaction of alumina, 498
Alumina–mild steel
Alumina–mild steel friction welded at lower rotational speed, 279
Aluminium
The effect of hot isostatic pressing on the fatigue behaviour of sand-cast A356-T6 and A204-T6 aluminum alloys, 231
Aluminum cylindrical bar
The effect of coatings on the thermo-mechanical response of cylindrical specimens during quenching, 39
Aluminum–copper alloys
The effect of time and temperature on the precipitation behavior and hardness of Al–4 wt%Cu alloy using design of experiments, 343
Annealing
Spark plasma sintering cobalt base superalloy strengthened by Y–Cr–O compound through high-energy milling, 111
Arc spot welding
Unified formulation for ultimate capacity of shear failure of arc spot welding using genetic programming, 117
Artificial precipitation
The effect of time and temperature on the precipitation behavior and hardness of Al–4 wt%Cu alloy using design of experiments, 343
A356-T6
The effect of hot isostatic pressing on the fatigue behaviour of sand-cast A356-T6 and A204-T6 aluminum alloys, 231
Austenite
Phase transformations across high strength dissimilar steel inertia friction weld, 48
Autocatalytic mechanism
Thermometric behaviour of cobalt in HNO_3 solutions, 139

Biomaterials
Modification of mechanical properties of sintered implant materials on the base of Co–Cr–Mo alloy, 199
Blow moulding
Manufacturing in blow molding: Time reduction and part quality improvement, 284
Blush
Influence of injection parameters on the formation of blush in injection moulding of PVC, 1
Boundary representation
A solid model-based off-line adaptive controller for feed rate scheduling for milling process, 384
Brass
Selection of optimal MQL and cutting conditions for enhancing machinability in turning of brass, 459

CAD
A volumetric approach for STL generation from 3D scanned products, 403
Carbon fiber
Carbon fiber reinforced silicon carbide mini-composites-solution approach, 434
Carbon monoxide
Effect of carbon monoxide on the carbothermal reduction and nitridation reaction of alumina, 498
Carbothermal reduction
Effect of carbon monoxide on the carbothermal reduction and nitridation reaction of alumina, 498
Cast Ti–47Al–2Cr–2Nb alloys
Centrifugal precision cast TiAl turbocharger wheel using ceramic mold, 492
Casting
Heat transfer in multi-block grid during solidification: Performance of Finite Differences and Finite Volume methods, 451
Casting defects
The effect of hot isostatic pressing on the fatigue behaviour of sand-cast A356-T6 and A204-T6 aluminum alloys, 231
Ceramic mold
Centrifugal precision cast TiAl turbocharger wheel using ceramic mold, 492

Elsevier B.V.
doi:10.1016/S0924-0136(08)00455-X

Chemical synthesis
A versatile method for preparing $FePO_4$ and study on its electrode performance in lithium ion batteries, 513
Chemical vapour deposition (CVD)
Fabrication of thin and dense nano-crystalline membranes on porous substrates, 248
Chip thickness
Chip thickness analysis for different tool motions. for adaptive feed rate, 213
Chisel edge
A study of computer-assisted analysis of effects of drill geometry and surface coating on forces and power in drilling, 130
Chiselling by fellows method
A comparative analysis of the geometrical surface texture of a real and virtual model of a tooth flank of a cylindrical gear, 331
Circular interpolation
Chip thickness analysis for different tool motions. for adaptive feed rate, 213
Coatings
Thermal-sprayed coatings on aluminium for mould tool protection and upgrade, 184
Cobalt
Thermometric behaviour of cobalt in HNO_3 solutions, 139
Cobalt base superalloy
Spark plasma sintering cobalt base superalloy strengthened by Y–Cr–O compound through high-energy milling, 111
Co–Cr–Mo-alloys
Modification of mechanical properties of sintered implant materials on the base of Co–Cr–Mo alloy, 199
Composite
Carbon fiber reinforced silicon carbide mini-composites-solution approach, 434
Composite materials
Modification of mechanical properties of sintered implant materials on the base of Co–Cr–Mo alloy, 199
Computer simulation
A study of die design of semi-solid die casting according to gate shape and solid fraction, 8
Computer simulation of gear generation
A comparative analysis of the geometrical surface texture of a real and virtual model of a tooth flank of a cylindrical gear, 331
Computer-assisted predictions
A study of computer-assisted analysis of effects of drill geometry and surface coating on forces and power in drilling, 130
Concurrent engineering
Manufacturing in blow molding: Time reduction and part quality improvement, 284
Constitutive relationship
Hot deformation behavior of a spray formed superalloy, 147
Control model
A flying gauge change model in tandem cold strip mill, 152
Convection–diffusion
3D filling simulation of injection molding based on the PG method, 475
Conventional deep drawing
Effect of process parameters on product surface finish and thickness variation in hydro-mechanical deep drawing, 169
Crash test
State of art of impact tensile test (ITT): Its historical development as a simulated crash test of industrial materials and presentation of new "ductile/brittle" transition diagrams, 313
Crystallization kinetics
Effect of Zr on glass-forming ability and crystallization kinetics of $Y_{56}Al_{24}Co_{20}$ metallic glass, 179
Cutoff pressure
Effect of process parameters on product surface finish and thickness variation in hydro-mechanical deep drawing, 169
Cutting force
Effect of cutting speed on the performance of coated and uncoated cutting tools in turning nodular cast iron, 80
Cutting performance
A study of computer-assisted analysis of effects of drill geometry and surface coating on forces and power in drilling, 130
Cylindrical gears
A comparative analysis of the geometrical surface texture of a real and virtual model of a tooth flank of a cylindrical gear, 331

3D rolling forming
Analysis of 3D rolling forming with generalized rigid-plastic boundaries approach, 425
Damage mechanism
Comparative study: Mechanical and metallurgical aspects of tailored welded blanks (TWBs), 440
Defective voids
Investigation into equal channel angular extrusion process of billet with internal defects, 419
Deformability
Hot deformation behavior of a spray formed superalloy, 147
Design of experiments
The effect of time and temperature on the precipitation behavior and hardness of Al–4 wt%Cu alloy using design of experiments, 343
An experimental study for optimization of electrical discharge turning (EDT) process, 350
Design optimisation
Innovative design of a hybrid tool for turning assisted with superficial cold forming, 357
Dilatometer determination
Dilatometry determination of phase transformation temperatures during heating of Nb bearing low carbon steels, 365
Dissimilar welding
Control of welding residual stress for dissimilar laser welded materials, 22
Dissolution and Passivation
Thermometric behaviour of cobalt in HNO_3 solutions, 139
Drill lips
A study of computer-assisted analysis of effects of drill geometry and surface coating on forces and power in drilling, 130
Drill point geometry
A study of computer-assisted analysis of effects of drill geometry and surface coating on forces and power in drilling, 130
Dynamic setup
A flying gauge change model in tandem cold strip mill, 152

Electrical discharge turning
An experimental study for optimization of electrical discharge turning (EDT) process, 350
Electrochemical properties
A versatile method for preparing $FePO_4$ and study on its electrode performance in lithium ion batteries, 513
Electronic materials
A versatile method for preparing $FePO_4$ and study on its electrode performance in lithium ion batteries, 513
Empirical model
Analysis of surface roughness parameters in turning of FRP tubes by PCD tool, 469
Endurance limit
Effect of multi-impacts on a PMMA sheet material, 206
EPC process
Optimization of tensile properties of evaporative pattern casting process through Taguchi's method, 59
Equal channel angular (ECA) extrusion
Investigation into equal channel angular extrusion process of billet with internal defects, 419
Erosion rate
A mathematical model to characterize effect of silica content in the boiler fly ash on erosion behaviour of boiler grade steel, 239
Expanded perlite aggregate
Effect of expanded perlite aggregate on the properties of lightweight concrete, 34

Failure
The effect of laser shock peening on the life and failure mode of a cold pilger die, 486
Fatigue
The effect of hot isostatic pressing on the fatigue behaviour of sand-cast A356-T6 and A204-T6 aluminum alloys, 231
FE
The effect of coatings on the thermo-mechanical response of cylindrical specimens during quenching, 39
Fe(Co)-based BMGs
Evaluation on the reliability of criterions for glass-forming ability of Fe(Co)-based bulk metallic glasses, 465
Fibre-reinforced plastics
Analysis of surface roughness parameters in turning of FRP tubes by PCD tool, 469
Filling simulation
3D filling simulation of injection molding based on the PG method, 475
Finite difference
Heat transfer in multi-block grid during solidification: Performance of Finite Differences and Finite Volume methods, 451
Finite element analysis
Numerical investigations on springback characteristics of aluminum sheet metal alloys in warm forming conditions, 370
Finite element method
Effect of plug on levelling of residual stress in tube drawing, 162
Finite volume
Heat transfer in multi-block grid during solidification: Performance of Finite Differences and Finite Volume methods, 451
Finite-element
The effect of coatings on the thermo-mechanical response of cylindrical specimens during quenching, 39
Flank wear
Effect of cutting speed on the performance of coated and uncoated cutting tools in turning nodular cast iron, 80
Flow rate
Influence of injection parameters on the formation of blush in injection moulding of PVC, 1
Fly ash
A mathematical model to characterize effect of silica content in the boiler fly ash on erosion behaviour of boiler grade steel, 239
Flying gauge change
A flying gauge change model in tandem cold strip mill, 152
Fracture mechanics
State of art of impact tensile test (ITT): Its historical development as a simulated crash test of industrial materials and presentation of new "ductile/brittle" transition diagrams, 313
Fragility parameter
Effect of Zr on glass-forming ability and crystallization kinetics of $Y_{56}Al_{24}Co_{20}$ metallic glass, 179
Free surface
Melt extraction of short metallic filaments: Fibre formation process revisited, 103
Free-form surface
Improved surface roughness as a result of free-form surface machining using self-organized neural network, 94
Free-surface roughening
Validation of FE simulation based on surface roughness model in micro-deep drawing, 89
Fresh and hardened properties
Effect of expanded perlite aggregate on the properties of lightweight concrete, 34
Friction
Microstructural, thermal and mechanical properties of HVOF sprayed Ni–Al-based bond coatings on stainless steel substrate, 221
Friction welding
Alumina–mild steel friction welded at lower rotational speed, 279

Gate shape
A study of die design of semi-solid die casting according to gate shape and solid fraction, 8
Generalized rigid-plastic boundaries
Analysis of 3D rolling forming with generalized rigid-plastic boundaries approach, 425
Genetic programming
Unified formulation for ultimate capacity of shear failure of arc spot welding using genetic programming, 117
GFA
Evaluation on the reliability of criterions for glass-forming ability of Fe(Co)-based bulk metallic glasses, 465
Glass-forming ability
Effect of Zr on glass-forming ability and crystallization kinetics of $Y_{56}Al_{24}Co_{20}$ metallic glass, 179
Glossiness
Evaluation of continuous grinding tests on some marble and limestone units with silicon carbide and diamond type abrasives, 264

Grain refinement
Dilatometry determination of phase transformation temperatures during heating of Nb bearing low carbon steels, 365
Grinding
Experimental validation of numerical thermal models for dry grinding, 269

Hardening
Grain refinement and strain hardening in IF steel during multi-axis compression: Experiment and modelling, 255
Hardness
The effect of time and temperature on the precipitation behavior and hardness of Al–4 wt%Cu alloy using design of experiments, 343
Heat treatment
Effect of heat treatment, lubricant and sintering temperature on dry sliding wear behavior of medium alloyed chromium PM steels, 192
High-energy milling
Spark plasma sintering cobalt base superalloy strengthened by Y–Cr–O compound through high-energy milling, 111
HIP
The effect of hot isostatic pressing on the fatigue behaviour of sand-cast A356-T6 and A204-T6 aluminum alloys, 231
Hobbing
A comparative analysis of the geometrical surface texture of a real and virtual model of a tooth flank of a cylindrical gear, 331
Hole-drilling method
Control of welding residual stress for dissimilar laser welded materials, 22
Hot isostatic pressing
The effect of hot isostatic pressing on the fatigue behaviour of sand-cast A356-T6 and A204-T6 aluminum alloys, 231
HVOF
Microstructural, thermal and mechanical properties of HVOF sprayed Ni–Al-based bond coatings on stainless steel substrate, 221
Hybrid tooling
Innovative design of a hybrid tool for turning assisted with superficial cold forming, 357
Hydrolysis
Synthesis of Ag nanoparticles by hydrolysis of Mg–Ag intermetallic compounds, 327
Hydro-mechanical deep drawing
Effect of process parameters on product surface finish and thickness variation in hydro-mechanical deep drawing, 169
Hydro-mechanical stretch forming
Improvement in formability of tailor welded blanks by application of counter pressure in biaxial stretch forming, 70

Image space representation
A solid model-based off-line adaptive controller for feed rate scheduling for milling process, 384
Impact crash test
Comparative study: Mechanical and metallurgical aspects of tailored welded blanks (TWBs), 440
Impact fatigue
Effect of multi-impacts on a PMMA sheet material, 206
Impact velocity
Effect of multi-impacts on a PMMA sheet material, 206
Imprint
Development of self-built multilayer aligner for imprint process, 502
Incremental sheet forming
Incremental forming of sandwich panels, 290
Indentation
Influence of the deposition techniques on the mechanical properties and microstructure of NiCrBSi coatings, 304
Microstructural, thermal and mechanical properties of HVOF sprayed Ni–Al-based bond coatings on stainless steel substrate, 221
Index of surface complexity (ISC)
Improved surface roughness as a result of free-form surface machining using self-organized neural network, 94
Inertia friction welding
Phase transformations across high strength dissimilar steel inertia friction weld, 48
Infrared
Experimental validation of numerical thermal models for dry grinding, 269
Injection molding
3D filling simulation of injection molding based on the PG method, 475
Injection mould tooling
Thermal-sprayed coatings on aluminium for mould tool protection and upgrade, 184
Injection pressure
Influence of injection parameters on the formation of blush in injection moulding of PVC, 1
Injection velocity
A study of die design of semi-solid die casting according to gate shape and solid fraction, 8
Integration
A volumetric approach for STL generation from 3D scanned products, 403
Interlayer materials
Alumina–mild steel friction welded at lower rotational speed, 279
Intermetallic compound
Synthesis of Ag nanoparticles by hydrolysis of Mg–Ag intermetallic compounds, 327
Inverse heat-transfer
The effect of coatings on the thermo-mechanical response of cylindrical specimens during quenching, 39
Ionic conducting membrane
Fabrication of thin and dense nano-crystalline membranes on porous substrates, 248
Iron phosphate
A versatile method for preparing $FePO_4$ and study on its electrode performance in lithium ion batteries, 513
ITT (impact tesile crash test)
State of art of impact tensile test (ITT): Its historical development as a simulated crash test of industrial materials and presentation of new "ductile/brittle" transition diagrams, 313

K10 carbide tool
Selection of optimal MQL and cutting conditions for enhancing machinability in turning of brass,459
Kerf deviation
Optimization of kerf quality during pulsed laser cutting of aluminium alloy sheet, 412
Kerf width
Optimization of kerf quality during pulsed laser cutting of aluminium alloy sheet, 412

Laser beam cutting
Optimization of kerf quality during pulsed laser cutting of aluminium alloy sheet, 412
Laser shock peening
The effect of laser shock peening on the life and failure mode of a cold pilger die, 486
LASER welding
State of art of impact tensile test (ITT): Its historical development as a simulated crash test of industrial materials and presentation of new "ductile/brittle" transition diagrams, 313
LASER welding process
Comparative study: Mechanical and metallurgical aspects of tailored welded blanks (TWBs), 440
Light-emitting devices
High quality p-type ZnO films grown by low pressure plasma-assisted MOCVD with N_2O rf plasma doping source, 481
Lightweight concrete
Effect of expanded perlite aggregate on the properties of lightweight concrete, 34
Lightweight materials
Numerical investigations on springback characteristics of aluminum sheet metal alloys in warm forming conditions, 370
Limiting dome height
Improvement in formability of tailor welded blanks by application of counter pressure in biaxial stretch forming, 70
Linear interpolation
Chip thickness analysis for different tool motions. for adaptive feed rate, 213
Linear regression
Evaluation on the reliability of criterions for glass-forming ability of Fe(Co)-based bulk metallic glasses, 465
Lithography
Development of self-built multilayer aligner for imprint process, 502
Lubricant
Effect of heat treatment, lubricant and sintering temperature on dry sliding wear behavior of medium alloyed chromium PM steels, 192

Material removal rate
An experimental study for optimization of electrical discharge turning (EDT) process, 350
Mathematical models
A mathematical model to characterize effect of silica content in the boiler fly ash on erosion behaviour of boiler grade steel, 239
Mechanical properties
Influence of the deposition techniques on the mechanical properties and microstructure of NiCrBSi coatings, 304
Modification of mechanical properties of sintered implant materials on the base of Co–Cr–Mo alloy, 99
Centrifugal precision cast TiAl turbocharger wheel using ceramic mold, 492
Melt extraction
Melt extraction of short metallic filaments: Fibre formation process revisited, 103
Metallic fibres
Melt extraction of short metallic filaments: Fibre formation process revisited, 103
Metallurgy of welded parts
Comparative study: Mechanical and metallurgical aspects of tailored welded blanks (TWBs), 440
Metalorganic chemical vapor deposition
High quality p-type ZnO films grown by low pressure plasma-assisted MOCVD with N_2O rf plasma doping source, 481
Micro-deep drawing
Validation of FE simulation based on surface roughness model in micro-deep drawing, 89
Microstructure
Influence of the deposition techniques on the mechanical properties and microstructure of NiCrBSi coatings, 304
Effect of heat treatment, lubricant and sintering temperature on dry sliding wear behavior of medium alloyed chromium PM steels, 192
Microstructural, thermal and mechanical properties of HVOF sprayed Ni–Al-based bond coatings on stainless steel substrate, 221
Grain refinement and strain hardening in IF steel during multi-axis compression: Experiment and modelling, 255
Centrifugal precision cast TiAl turbocharger wheel using ceramic mold, 492
Milling
Chip thickness analysis for different tool motions. for adaptive feed rate, 213
Modelling
Grain refinement and strain hardening in IF steel during multi-axis compression: Experiment and modelling, 255
Mold multi-piece design
Centrifugal precision cast TiAl turbocharger wheel using ceramic mold, 492
MQL
Selection of optimal MQL and cutting conditions for enhancing machinability in turning of brass, 459
MRR
A solid model-based off-line adaptive controller for feed rate scheduling for milling process, 384
Multi-block grid
Heat transfer in multi-block grid during solidification: Performance of Finite Differences and Finite Volume methods, 451
Multilayer alignment
Development of self-built multilayer aligner for imprint process, 502

Nanocomposite
Investigation of Ni nanocrystallization and the effect of Al_2O_3 addition by high-energy ball milling, 125
Nanocrystalline, High-energy ball milling
Investigation of Ni nanocrystallization and the effect of Al_2O_3 addition by high-energy ball milling, 125
NC verification
A solid model-based off-line adaptive controller for feed rate scheduling for milling process, 384
Nd:YAG
Optimization of kerf quality during pulsed laser cutting of aluminium alloy sheet, 412
Neural network (NN)
Improved surface roughness as a result of free-form surface machining using self-organized neural network, 94
Neuron
Improved surface roughness as a result of free-form surface machining using self-organized neural network, 94

New ductile/brittle temperature transition curves
State of art of impact tensile test (ITT): Its historical development as a simulated crash test of industrial materials and presentation of new "ductile/brittle" transition diagrams, 313
NiAl
Microstructural, thermal and mechanical properties of HVOF sprayed Ni–Al-based bond coatings on stainless steel substrate, 221
NiCrBSi
Influence of the deposition techniques on the mechanical properties and microstructure of NiCrBSi coatings, 304
Niobium
Dilatometry determination of phase transformation temperatures during heating of Nb bearing low carbon steels, 365
Nitric acid
Thermometric behaviour of cobalt in HNO_3 solutions, 139
Nodular cast iron
Effect of cutting speed on the performance of coated and uncoated cutting tools in turning nodular cast iron, 80
Numerical modelling
Manufacturing in blow molding: Time reduction and part quality improvement, 284

Octree representation
A solid model-based off-line adaptive controller for feed rate scheduling for milling process, 384
Optimisation
Manufacturing in blow molding: Time reduction and part quality improvement, 284
Optimization
Optimization of tensile properties of evaporative pattern casting process through Taguchi's method, 59

Parameter γ
Evaluation on the reliability of criterions for glass-forming ability of Fe(Co)-based bulk metallic glasses, 465
Phase transformations
Phase transformations across high strength dissimilar steel inertia friction weld, 48
Photoluminescence
High quality p-type ZnO films grown by low pressure plasma-assisted MOCVD with N_2O rf plasma doping source, 481
Photoresist
Development of self-built multilayer aligner for imprint process, 502
Pilger die
The effect of laser shock peening on the life and failure mode of a cold pilger die, 486
Plug drawing
Effect of plug on levelling of residual stress in tube drawing, 162
PMDA
Rheological characterisation of recycled poly(ethylene terephthalate) modified by reactive extrusion, 397
PMMA
Effect of multi-impacts on a PMMA sheet material, 206
Porous substrate
Fabrication of thin and dense nano-crystalline membranes on porous substrates, 248
Power
A study of computer-assisted analysis of effects of drill geometry and surface coating on forces and power in drilling, 130
Pre-bulging pressure
Effect of process parameters on product surface finish and thickness variation in hydro-mechanical deep drawing, 169
Precipitation heat treatment
The effect of time and temperature on the precipitation behavior and hardness of Al–4 wt%Cu alloy using design of experiments, 343
Predicted thrust
A study of computer-assisted analysis of effects of drill geometry and surface coating on forces and power in drilling, 130
Process element (PE)
Improved surface roughness as a result of free-form surface machining using self-organized neural network, 94
Process simulation
Manufacturing in blow molding: Time reduction and part quality improvement, 284
Profile curves
A technical note on profile curves design of tooth-shaped rolls, 508
PSPG
3D filling simulation of injection molding based on the PG method, 475
p-type doping
High quality p-type ZnO films grown by low pressure plasma-assisted MOCVD with N_2O rf plasma doping source, 481
PVC
Influence of injection parameters on the formation of blush in injection moulding of PVC, 1

Quenching
The effect of coatings on the thermo-mechanical response of cylindrical specimens during quenching, 39

Rake angle distributions
A study of computer-assisted analysis of effects of drill geometry and surface coating on forces and power in drilling, 130
Rapid prototyping
A volumetric approach for STL generation from 3D scanned products, 403
Rare-earth-based metallic glass
Effect of Zr on glass-forming ability and crystallization kinetics of $Y_{56}Al_{24}Co_{20}$ metallic glass, 179
Reactive extrusion
Rheological characterisation of recycled poly(ethylene terephthalate) modified by reactive extrusion, 397
Recycled PET
Rheological characterisation of recycled poly(ethylene terephthalate) modified by reactive extrusion, 397
Residual stress
Effect of plug on levelling of residual stress in tube drawing, 162
The effect of laser shock peening on the life and failure mode of a cold pilger die, 486
Residual stresses
Control of welding residual stress for dissimilar laser welded materials, 22
The effect of coatings on the thermo-mechanical response of cylindrical specimens during quenching, 39

Retardation
Effect of carbon monoxide on the carbothermal reduction and nitridation reaction of alumina, 498
Reverse engineering
A volumetric approach for STL generation from 3D scanned products, 403
Rheological properties
Rheological characterisation of recycled poly(ethylene terephthalate) modified by reactive extrusion, 397
Rigid-plastic finite element
Investigation into equal channel angular extrusion process of billet with internal defects, 419
Roll gap
A flying gauge change model in tandem cold strip mill, 152
Roll speed
A flying gauge change model in tandem cold strip mill, 152
Rotational speed
Alumina–mild steel friction welded at lower rotational speed, 279
Roughness
Evaluation of continuous grinding tests on some marble and limestone units with silicon carbide and diamond type abrasives, 264

Sandwich panels
Incremental forming of sandwich panels, 290
Self-organized Kohonen neural network (SOKN)
Improved surface roughness as a result of free-form surface machining using self-organized neural network, 94
Semi-solid processing
A study of die design of semi-solid die casting according to gate shape and solid fraction, 8
Severe plastic deformation
Grain refinement and strain hardening in IF steel during multi-axis compression: Experiment and modelling, 255
Shear failure
Unified formulation for ultimate capacity of shear failure of arc spot welding using genetic programming, 117
SiC
Carbon fiber reinforced silicon carbide mini-composites-solution approach, 434
Silica content
A mathematical model to characterize effect of silica content in the boiler fly ash on erosion behaviour of boiler grade steel, 239
Simultaneous optimization
Optimization of kerf quality during pulsed laser cutting of aluminium alloy sheet, 412
Solid fraction
A study of die design of semi-solid die casting according to gate shape and solid fraction, 8
Solid modeling
A solid model-based off-line adaptive controller for feed rate scheduling for milling process, 384
Solid solution retardation
Dilatometry determination of phase transformation temperatures during heating of Nb bearing low carbon steels, 365
Solidification
Heat transfer in multi-block grid during solidification: Performance of Finite Differences and Finite Volume methods, 451
Solution approach
Carbon fiber reinforced silicon carbide mini-composites-solution approach, 434
Spark plasma sintering
Spark plasma sintering cobalt base superalloy strengthened by Y–Cr–O compound through high-energy milling, 111
Specific cutting force
Selection of optimal MQL and cutting conditions for enhancing machinability in turning of brass, 459
Spray deposition techniques
Influence of the deposition techniques on the mechanical properties and microstructure of NiCrBSi coatings, 304
Spray forming
Hot deformation behavior of a spray formed superalloy, 147
Springback
Numerical investigations on springback characteristics of aluminum sheet metal alloys in warm forming conditions, 370
State variable
The effect of coatings on the thermo-mechanical response of cylindrical specimens during quenching, 39
Steel grades
A mathematical model to characterize effect of silica content in the boiler fly ash on erosion behaviour of boiler grade steel, 239
Stone grinding
Evaluation of continuous grinding tests on some marble and limestone units with silicon carbide and diamond type abrasives, 264
Strain distribution
Improvement in formability of tailor welded blanks by application of counter pressure in biaxial stretch forming, 70
Strain rate
Hot deformation behavior of a spray formed superalloy, 147
Superalloy
Hot deformation behavior of a spray formed superalloy, 147
Superficial cold forming
Innovative design of a hybrid tool for turning assisted with superficial cold forming, 357
SUPG
3D filling simulation of injection molding based on the PG method, 475
Surface coating
The effect of coatings on the thermo-mechanical response of cylindrical specimens during quenching, 39
Surface coatings
A study of computer-assisted analysis of effects of drill geometry and surface coating on forces and power in drilling, 130
Surface finish
Effect of cutting speed on the performance of coated and uncoated cutting tools in turning nodular cast iron, 80
Effect of process parameters on product surface finish and thickness variation in hydro-mechanical deep drawing, 169
Surface roughness
Validation of FE simulation based on surface roughness model in micro-deep drawing, 89

Microstructural, thermal and mechanical properties of HVOF sprayed Ni–Al-based bond coatings on stainless steel substrate, 221
Selection of optimal MQL and cutting conditions for enhancing machinability in turning of brass, 459
Surface roughness parameters
Analysis of surface roughness parameters in turning of FRP tubes by PCD tool, 469

Taguchi
An experimental study for optimization of electrical discharge turning (EDT) process, 350
Taguchi approach
Control of welding residual stress for dissimilar laser welded materials, 22
Taguchi method
Selection of optimal MQL and cutting conditions for enhancing machinability in turning of brass, 459
Optimization of kerf quality during pulsed laser cutting of aluminium alloy sheet, 412
Taguchi technique
Optimization of tensile properties of evaporative pattern casting process through Taguchi's method, 59
Tailored welded blanks
Improvement in formability of tailor welded blanks by application of counter pressure in biaxial stretch forming, 70
Comparative study: Mechanical and metallurgical aspects of tailored welded blanks (TWBs), 440
Tailored blanks
State of art of impact tensile test (ITT): Its historical development as a simulated crash test of industrial materials and presentation of new "ductile/brittle" transition diagrams, 313
Tandem cold strip mill
A flying gauge change model in tandem cold strip mill, 152
Temperature measurement
Experimental validation of numerical thermal models for dry grinding, 269
Tensile properties
Optimization of tensile properties of evaporative pattern casting process through Taguchi's method, 59
A mathematical model to characterize effect of silica content in the boiler fly ash on erosion behaviour of boiler grade steel, 239
Tensile strength
Carbon fiber reinforced silicon carbide mini-composites-solution approach, 434
Testing apparatus
Effect of multi-impacts on a PMMA sheet material, 206
TFT-LCD
Development of self-built multilayer aligner for imprint process, 502
Thermal
Microstructural, thermal and mechanical properties of HVOF sprayed Ni–Al-based bond coatings on stainless steel substrate, 221
Thermal modeling
Experimental validation of numerical thermal models for dry grinding, 269
Thermal spray
Thermal-sprayed coatings on aluminium for mould tool protection and upgrade, 184
Thermal stability
Effect of Zr on glass-forming ability and crystallization kinetics of $Y_{56}Al_{24}Co_{20}$ metallic glass, 179
Thermometric
Thermometric behaviour of cobalt in HNO_3 solutions, 139
Thickness distribution
Effect of process parameters on product surface finish and thickness variation in hydro-mechanical deep drawing, 169
Tooth flank surface stereometry
A comparative analysis of the geometrical surface texture of a real and virtual model of a tooth flank of a cylindrical gear, 331
Tooth flank surface topography
A comparative analysis of the geometrical surface texture of a real and virtual model of a tooth flank of a cylindrical gear, 331
Tooth trajectories
Chip thickness analysis for different tool motions. for adaptive feed rate, 213
Tooth-shaped rolls
A technical note on profile curves design of tooth-shaped rolls, 508
Torque
A study of computer-assisted analysis of effects of drill geometry and surface coating on forces and power in drilling, 130
Transverse rupture strength
Effect of heat treatment, lubricant and sintering temperature on dry sliding wear behavior of medium alloyed chromium PM steels, 192
Tube drawing
Effect of plug on levelling of residual stress in tube drawing, 162
Turning
Innovative design of a hybrid tool for turning assisted with superficial cold forming, 357
Selection of optimal MQL and cutting conditions for enhancing machinability in turning of brass, 459
Analysis of surface roughness parameters in turning of FRP tubes by PCD tool, 469

Ultimate capacity
Unified formulation for ultimate capacity of shear failure of arc spot welding using genetic programming, 117
Utility concept
Selection of optimal MQL and cutting conditions for enhancing machinability in turning of brass, 459

Volumetric NC simulation
A solid model-based off-line adaptive controller for feed rate scheduling for milling process, 384

Warm forming
Numerical investigations on springback characteristics of aluminum sheet metal alloys in warm forming conditions, 370
Wear
Effect of heat treatment, lubricant and sintering temperature on dry sliding wear behavior of medium alloyed chromium PM steels, 192

Microstructural, thermal and mechanical properties of HVOF sprayed Ni–Al-based bond coatings on stainless steel substrate, 221
Weld line movement
Improvement in formability of tailor welded blanks by application of counter pressure in biaxial stretch forming, 70
Wetting
Melt extraction of short metallic filaments: Fibre formation process revisited, 103
Wholly corrugated webs
A technical note on profile curves design of tooth-shaped rolls, 508
Width spread
Analysis of 3D rolling forming with generalized rigid-plastic boundaries approach, 425

X-ray diffraction
Phase transformations across high strength dissimilar steel inertia friction weld, 48

Zinc oxide films
High quality p-type ZnO films grown by low pressure plasma-assisted MOCVD with N_2O rf plasma doping source, 481

ELSEVIER

Volume 204, Issues 1–3, 11 August 2008

Journal of
Materials
Processing
Technology

www.elsevier.com/locate/jmatprotec

Contents

Influence of injection parameters on the formation of blush in injection moulding of PVC 1
J. Lladó, B. Sánchez

A study of die design of semi-solid die casting according to gate shape and solid fraction 8
C.G. Kang, S.M. Lee, B.-M. Kim

Control of welding residual stress for dissimilar laser welded materials 22
E.M. Anawa, A.G. Olabi

Effect of expanded perlite aggregate on the properties of lightweight concrete 34
İ.B. Topçu, B. Işıkdağ

The effect of coatings on the thermo-mechanical response of cylindrical specimens during quenching 39
P. Ulysse, R.W. Schultz

Phase transformations across high strength dissimilar steel inertia friction weld 48
R. Moat, M. Karadge, M. Preuss, S. Bray, M. Rawson

Optimization of tensile properties of evaporative pattern casting process through Taguchi's method 59
S. Kumar, P. Kumar, H.S. Shan

Improvement in formability of tailor welded blanks by application of counter pressure in biaxial stretch forming 70
S.K. Panda, D.R. Kumar

Effect of cutting speed on the performance of coated and uncoated cutting tools in turning nodular cast iron 80
R. Yigit, E. Celik, F. Findik, S. Koksal

Validation of FE simulation based on surface roughness model in micro-deep drawing 89
K. Manabe, T. Shimizu, H. Koyama, M. Yang, K. Ito

Improved surface roughness as a result of free-form surface machining using self-organized neural network 94
M. Korosec, J. Kopac

Melt extraction of short metallic filaments: Fibre formation process revisited 103
A. Cramer, G. Gerbeth

Spark plasma sintering cobalt base superalloy strengthened by Y–Cr–O compound through high-energy milling 111
C.F. Tang, F. Pan, X.H. Qu, C.C. Jia, B.H. Duan, X.B. He

Unified formulation for ultimate capacity of shear failure of arc spot welding using genetic programming 117
A. Cevik

Investigation of Ni nanocrystallization and the effect of Al_2O_3 addition by high-energy ball milling 125
T. Mousavi, F. Karimzadeh, M.H. Abbasi, M.H. Enayati

A study of computer-assisted analysis of effects of drill geometry and surface coating on forces and power in drilling 130
J. Audy

Thermometric behaviour of cobalt in HNO_3 solutions 139
S.M. Abd El Haleem, E.E. Abd El Aal

(Contents continued on page I)

0924-0136(20080811)204:1/3;1-D

(Contents continued from OBC)

Hot deformation behavior of a spray formed superalloy 147
F.W. Kang, G.Q. Zhang, J.F. Sun, Z. Li, J. Shen

A flying gauge change model in tandem cold strip mill 152
J.S. Wang, Z.Y. Jiang, A.K. Tieu, X.H. Liu, G.D. Wang

Effect of plug on levelling of residual stress in tube drawing 162
T. Kuboki, K. Nishida, T. Sakaki, M. Murata

Effect of process parameters on product surface finish and thickness variation in hydro-mechanical deep drawing 169
S.K. Singh, D. Ravi Kumar

Effect of Zr on glass-forming ability and crystallization kinetics of $Y_{56}Al_{24}Co_{20}$ metallic glass 179
S. He, Y. Liu, B. Huang, Z. Li, H. Wu

Thermal-sprayed coatings on aluminium for mould tool protection and upgrade 184
G.J. Gibbons, R.G. Hansell

Effect of heat treatment, lubricant and sintering temperature on dry sliding wear behavior of medium alloyed chromium PM steels 192
A. Babakhani, A. Haerian, M. Ghambri

Modification of mechanical properties of sintered implant materials on the base of Co–Cr–Mo alloy 199
M. Grądzka-Dahlke, J.R. Dąbrowski, B. Dąbrowski

Effect of multi-impacts on a PMMA sheet material 206
S.K. Sahoo, V.V. Silberschmidt

Chip thickness analysis for different tool motions. for adaptive feed rate 213
L. Saï, W. Bouzid, A. Zghal

Microstructural, thermal and mechanical properties of HVOF sprayed Ni–Al-based bond coatings on stainless steel substrate 221
O. Culha, E. Celik, N.F. Ak Azem, I. Birlik, M. Toparli, A. Turk

The effect of hot isostatic pressing on the fatigue behaviour of sand-cast A356-T6 and A204-T6 aluminum alloys 231
L. Ceschini, A. Morri, G. Sambogna

A mathematical model to characterize effect of silica content in the boiler fly ash on erosion behaviour of boiler grade steel 239
S.K. Das, K.M. Godiwalla, S.S. Hegde, S.P. Mehrotra, P.K. Dey

Fabrication of thin and dense nano-crystalline membranes on porous substrates 248
V. Faucheux, M. Audier, L. Rapenne, S. Pignard

Grain refinement and strain hardening in IF steel during multi-axis compression: Experiment and modelling. 255
H. Petryk, S. Stupkiewicz, R. Kuziak

Evaluation of continuous grinding tests on some marble and limestone units with silicon carbide and diamond type abrasives 264
K. Görgülü, A. Ceylanoğlu

Experimental validation of numerical thermal models for dry grinding 269
D. Anderson, A. Warkentin, R. Bauer

Alumina–mild steel friction welded at lower rotational speed 279
M.Z. Noh, L.B. Hussain, Z.A. Ahmad

Manufacturing in blow molding: Time reduction and part quality improvement. 284
A. Attar, N. Bhuiyan, V. Thomson

Incremental forming of sandwich panels 290
K.P. Jackson, J.M. Allwood, M. Landert

Influence of the deposition techniques on the mechanical properties and microstructure of NiCrBSi coatings. . . 304
T. Gómez-del Río, M.A. Garrido, J.E. Fernández, M. Cadenas, J. Rodríguez

State of art of impact tensile test (ITT): Its historical development as a simulated crash test of industrial materials and presentation of new "ductile/brittle" transition diagrams 313
E. Bayraktar, D. Kaplan, F. Schmidt, H. Paqueton, M. Grumbach

Synthesis of Ag nanoparticles by hydrolysis of Mg–Ag intermetallic compounds 327
H. Wang, Y. Lou, D.O. Northwood

A comparative analysis of the geometrical surface texture of a real and virtual model of a tooth flank of a cylindrical gear 331
J. Michalski, L. Skoczylas

The effect of time and temperature on the precipitation behavior and hardness of Al–4 wt%Cu alloy using design of experiments 343
A.M. Hassan, O.M. Bataineh, K.M. Abed

An experimental study for optimization of electrical discharge turning (EDT) process 350
P. Matoorian, S. Sulaiman, M.M.H.M. Ahmad

Innovative design of a hybrid tool for turning assisted with superficial cold forming 357
D.A. Axinte, Y.Y. Cao

Dilatometry determination of phase transformation temperatures during heating of Nb bearing low carbon steels 365
A.I.Z. Farahat

Numerical investigations on springback characteristics of aluminum sheet metal alloys in warm forming conditions 370
H.S. Kim, M. Koç

A solid model-based off-line adaptive controller for feed rate scheduling for milling process 384
K.P. Karunakaran, R. Shringi

Rheological characterisation of recycled poly(ethylene terephthalate) modified by reactive extrusion 397
F. Daver, R. Gupta, E. Kosior

A volumetric approach for STL generation from 3D scanned products 403
L.M. Galantucci, G. Percoco, U. Dal Maso

Optimization of kerf quality during pulsed laser cutting of aluminium alloy sheet 412
A.K. Dubey, V. Yadava

Investigation into equal channel angular extrusion process of billet with internal defects 419
D.-C. Chen, C.-P. Chen

Analysis of 3D rolling forming with generalized rigid-plastic boundaries approach 425
J.-P. Wang, W.-C. Kao, H.-D. Lee, J. Wang

Carbon fiber reinforced silicon carbide mini-composites-solution approach 434
N. Padmavathi, J. Subrahmanyam, K.K. Ray, R. Mohanrao, P. Ghosal, S. Kumari

Comparative study: Mechanical and metallurgical aspects of tailored welded blanks (TWBs) 440
E. Bayraktar, D. Kaplan, B.S. Yilbas

Heat transfer in multi-block grid during solidification: Performance of Finite Differences and Finite Volume methods 451
A. Rouboa, E. Monteiro

Selection of optimal MQL and cutting conditions for enhancing machinability in turning of brass 459
V.N. Gaitonde, S.R. Karnik, J.P. Davim

Evaluation on the reliability of criterions for glass-forming ability of Fe(Co)-based bulk metallic glasses ... 465
X. Liang, T. Erenc-Sedziak, M. Kowalczyk, T. Kulik, B. Xu

Analysis of surface roughness parameters in turning of FRP tubes by PCD tool 469
K. Palanikumar, F. Mata, J.P. Davim

3D filling simulation of injection molding based on the PG method 475
H. Zhou, B. Yan, Y. Zhang

High quality p-type ZnO films grown by low pressure plasma-assisted MOCVD with N_2O rf plasma doping source 481
T. Yang, J. Bian, H. Liang, J. Sun, X. Wang, W. Liu, Y. Chang, G. Du

The effect of laser shock peening on the life and failure mode of a cold pilger die 486
C.A. Lavender, S.-T. Hong, M.T. Smith, R.T. Johnson, D. Lahrman

Centrifugal precision cast TiAl turbocharger wheel using ceramic mold 492
W. Shouren, G. Peiquan, Y. Liying

Effect of carbon monoxide on the carbothermal reduction and nitridation reaction of alumina 498
H.U. Joo, W.-S. Jung

Development of self-built multilayer aligner for imprint process 502
C.T. Pan, R.H. Cheng

A technical note on profile curves design of tooth-shaped rolls 508
J. Ma, W. Zhang

A versatile method for preparing $FePO_4$ and study on its electrode performance in lithium ion batteries .. 513
Y. Xu, Y. Lu, P. Yin, L. Yan, Z. Yang, R. Yang

Author index 520

Subject index 522